MODELING INELASTIC DEFORMATION OF SINGLE CRYSTAL SUPERALLOYS WITH ACCOUNT OF γ / γ' PHASES EVOLUTION

A.I. Grishchenko[1*], A.S. Semenov[1], L.B. Getsov[2]

[1]Peter the Great St. Petersburg Polytechnic University, Polytechnicheskaya 29, St. Petersburg, Russia

[2]Polzunov Central Boiler and Turbine Institute, Atamanskaya 3, St. Petersburg, Russia

*e-mail: gai-gr@yandex.ru

Annotation. Using single-crystal nickel-base superalloys for the gas turbine blades allows significantly increase the operating temperature and consequently the economy of gas turbine engine. At the microscopic level, the single-crystal nickel base alloys are structures consisting of two phases: γ'-phase, forming on the basis of Ni_3Al, which is dispersed in a matrix of γ-phase, representing a solid solution of alloying elements in nickel. On the basis of finite element homogenization the analysis of the influence of phase composition on the stress-strain diagram, as well as study the effect of the shape evolution of γ'-inclusion, occurring during the formation of raft structures, on the creep curves are performed. The results of simulations demonstrate a good agreement with experimental data for a single crystal nickel-base superalloy ZhS32.

1. Introduction

The blades of modern gas turbines must have a very high resistance against the high temperature inelastic deformation, so single-crystal nickel-base superalloys are widely used for blade production.

The high temperature strength, toughness and durability of single-crystal nickel-base superalloys is attributed to the two-phase composite microstructure consisting of a γ- matrix and of γ'- precipitates (Fig. 1a). Cubic γ'- precipitates (Ni_3Al) have a typical size of 0.5 μm, and are more or less regularly distributed in a Ni-matrix (γ-phase). The typical distance between the precipitates is only 60 nm [1]. Single-crystal nickel-based alloys have a tendency to change the microstructure during operating at the high-temperature creep. Initially the cubic γ' phase particles are spliced together in a plate, perpendicular to the loading direction.
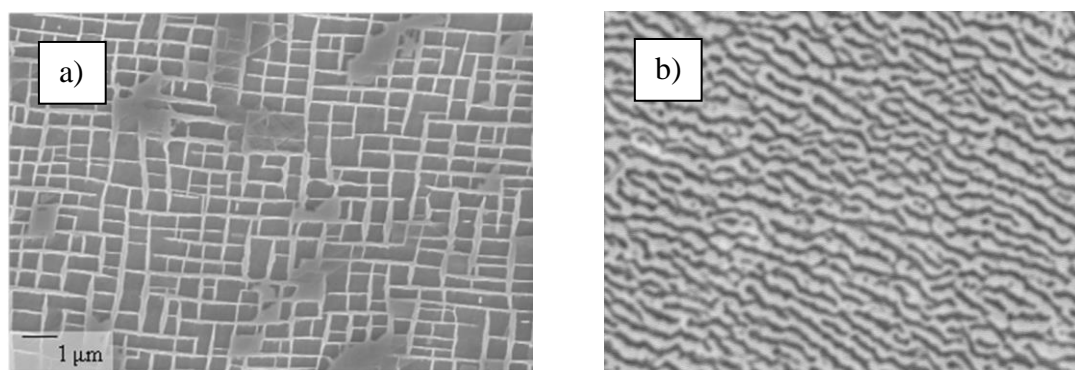

Fig. 1. Nickel-based superalloy microstructure: a) initial [1], b) after rafting [2].

Nowadays there is a wide range of phenomenological and physical material models for the simulation of inelastic behavior [3] and thermal fatigue [4, 5] of single-crystal turbine

blades. Most of models (see for example [6, 7]) are formulated on a macroscopic level and they do not take into account two-phase structure of the nickel base superalloys. Several models [8, 9] take into account the microstructural morphology (shapes and sizes of both phases), but their use requires great computation efforts for the modeling real turbine blades. The intermediate approach based on using micromechanically motivated phenomenological models obtained by homogenization is considered in the paper.

2. Representative volume element

The effective mechanical properties are defined on the base of finite element (FE) homogenization within the representative volume element (RVE) of the material. The RVE can be introduced for the material with a statistically uniform distribution (ergodic hypothesis) taking into account the scale separability of heterogeneities. In this case the least volume containing all the a priori statistical information on the distribution and morphology of the material heterogeneities can be correctly introduced. The three-dimensional variants of idealized RVE (whole and 1/8 unit cell), which are used below in FE computations, are presented in Fig. 2 by the rectangular γ' inclusion with rounded edges embedded in γ matrix.
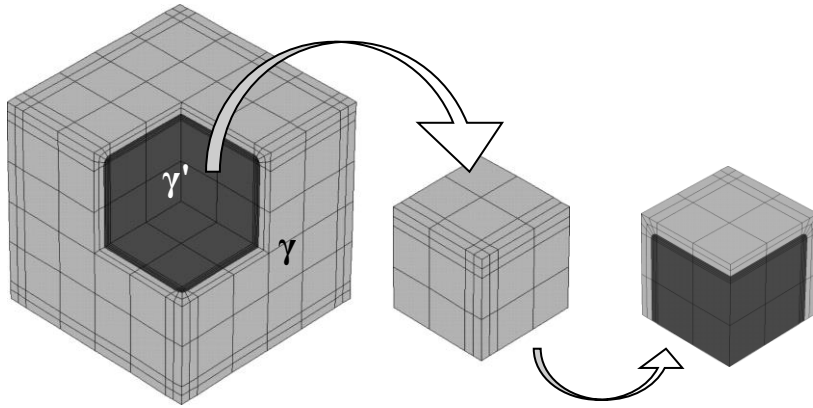

Fig. 2. FE model of two-phase RVE of nickel-base superalloy.

3. Constitutive equations

For the prediction of stress-strain state of both two-phase RVE and single-crystal blades it is rational to use micromechanical (physical) models of inelastic deformation, taking into account that the inelastic deformation occur in accordance with the slipping in the active slip systems.

It is assumed that plastic flow occurs as a result of possible slip in N slip systems, which are characterized by a normal to α^{th} slip plane $\mathbf{m}^{\alpha}$ and a slip direction $\mathbf{s}^{\alpha}$ ($\alpha=1,\dots,N$). For the considered case of single crystals with face-centered cubic lattice we have $N=12$ octahedral slip systems $\{111\}\langle 011\rangle$. The description of inelastic deformation processes for large strains is based on application of the concept of multiplicative decomposition of the strain gradient $\mathbf{F}$:

$$\mathbf{F} = \mathbf{F}^* \cdot \mathbf{F}^p , \tag{1}$$

where the plastic part of velocity gradient is defined by the equations

$$\mathbf{L}^p = \dot{\mathbf{F}}^p \cdot \mathbf{F}^{p^{-1}} = \sum_{\alpha=1}^{N} \dot{\gamma}^{\alpha} \mathbf{s}^{\alpha} \mathbf{m}^{\alpha} , \qquad \dot{\gamma}^{\alpha} = f(\tau^{\alpha},\dots) , \qquad \tau^{\alpha} = \boldsymbol{\sigma} \cdot\cdot\, \mathbf{s}^{\alpha} \mathbf{m}^{\alpha} \tag{2}$$

and elastic part is defined using equations

$$\mathbf{E}^* = \tfrac{1}{2}\left(\mathbf{C}^* - \mathbf{1}\right) = \tfrac{1}{2}\left(\mathbf{F}^* \cdot \mathbf{F}^{*^T} - \mathbf{1}\right), \qquad \mathbf{S}^* = {}^4\mathbf{D}\cdot\cdot\,\mathbf{E}^* , \qquad \mathbf{S}^* = J\mathbf{F}^{*^{-1}} \cdot \boldsymbol{\sigma} \cdot \mathbf{F}^{*^{-T}} . \tag{3}$$

In equations (2) and (3) $\boldsymbol{\sigma}$ and $\mathbf{S}^*$ denote Cauchy and second Piola-Kirchhoff stress

tensors respectively; $\mathbf{E}^*$ is a Green-Lagrangian strain tensor, $^4\mathbf{D}$ is a tensor of elastic moduli.

For the creep model multipliers $\dot{\gamma}^\alpha$ that characterize inelastic deformation intensity in α-slip system are calculated based on the equation:

$$\dot{\gamma}^\alpha = A|\tau^\alpha|^n sign(\tau^\alpha),\tag{4}$$

where A and n are material parameters depending on a temperature.

For the elasto-plastic model multipliers $\dot{\gamma}^\alpha$ are calculated based on the yield criteria:

$$f^\alpha = |\tau^\alpha| - R^\alpha - \tau_0 = 0,\tag{5}$$

where the variables that characterize isotropic hardening, are defined by equations [10]:

$$R^\alpha = bQ\sum_\beta h^{\alpha\beta}r^\beta, \qquad \dot{r}^\alpha = (1-br^\alpha)\dot{\gamma}^\alpha, \qquad h^{\alpha\beta} = H[q+(1-q)\delta_{ab}],\tag{6}$$

where b, Q, H and q are material parameters, coefficients $h^{\alpha,\beta}$ are introduced for account of the latent hardening [11].

The stress-state analysis of RVE is performed using the finite element software package PANTOCRATOR [12], where the constitutive equations (1)-(4) have been implemented.

3. Results of finite element modeling of deformation processes of RVE

Influence of γ' phase volume fraction on the creep. In order to evaluate the influence of γ' phase volume fraction on the creep behavior of RVE the FE computation are carried out with different γ' phase volume fractions from 0 % to 100 %. Used in computations the finite element models are shown in Fig. 3. The results of FE homogenization of RVE creep are shown in Fig. 4. Creep constants for (4) used in computations for alloy ZhS32 at 1050 °C are given in Table 1.

Table 1. Creep constants for (4) used in computations for alloy ZhS32 at 1050 °C.

constants	units	γ-phase	γ'-phase
A	(MPa)$^{-n}$/s	$0.61\cdot10^{-51}$	$1.99\cdot10^{-41}$
n	-	5.36	4.24

Multivariant computational experiments show that the increasing of the γ' phase volume fraction leads to decreasing the creep rate (see Fig. 4). The comparison of finite element results with experimental data [2] for the creep curves of alloy ZhS32 under 1050 °C for 58 % and 70 % γ' phase volume fractions shows a good agreement (see Fig. 5).
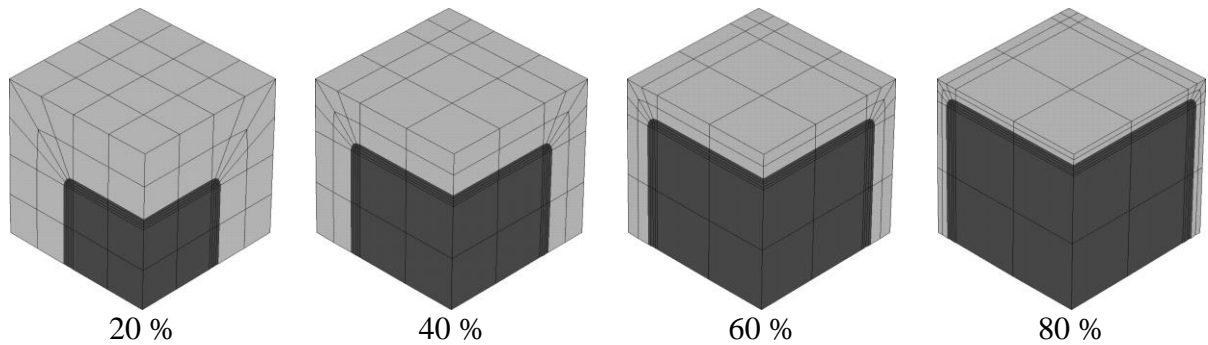

| 20 % | 40 % | 60 % | 80 % |

Fig. 3. Finite element models of RVE for different γ' phase volume fractions.
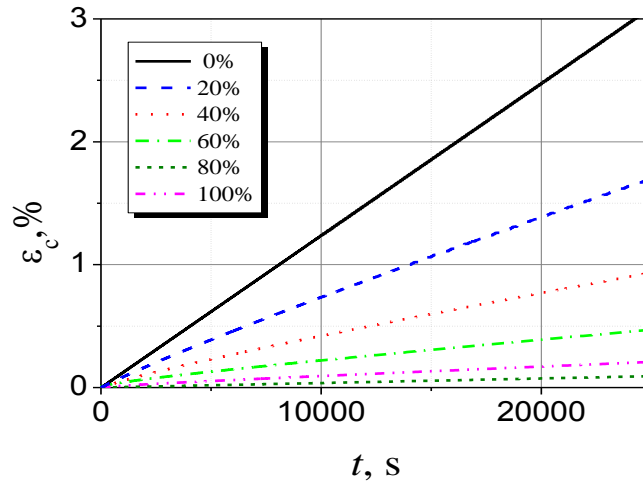
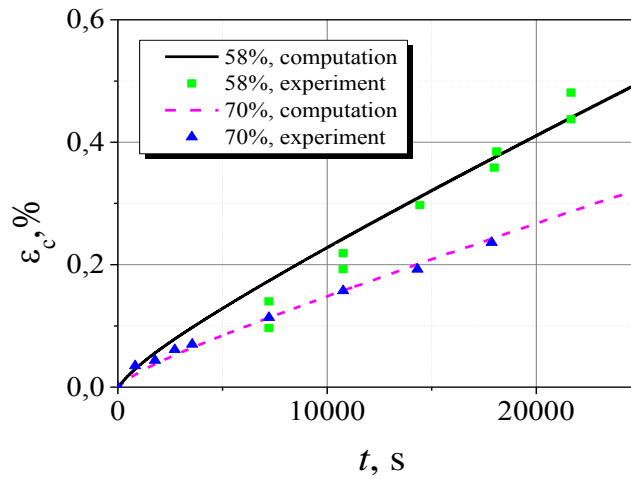**Fig. 4.** Creep curves for the different γ' volume fractions.

Fig. 5. Comparison of finite element results with experimental data [2].

Influence of γ' phase volume fraction on the plastic behavior. In order to evaluate the influence of γ' phase volume fraction on plastic behavior of RVE the FE computations are carried out with different γ' phase volumes varying from 0 % to 100 %. Plastic constants for (5)-(6) used in computations for alloy CMSX2 are shown in Table 2. The results of numerical computations of uniaxial tension of RVE is shown in Fig. 6. Increasing the proportion of γ' phase leads to growth of the yield stress and decrease of deformation diagram slope that qualitative und quantitative corresponds to that effects observed in experiments [8].

Table 2. Plastic constants for (5)-(6) used in FE computations for alloy CMSX2 at 650 ºC.

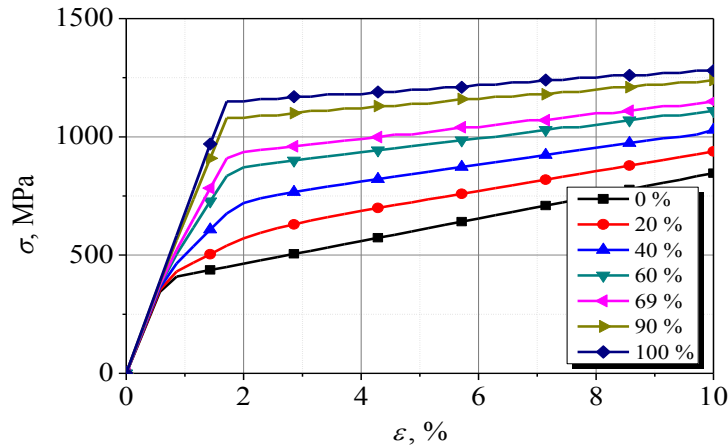| constants	units	γ-phase	γ'-phase
$\sigma_Y = \tau_0 \sqrt{2}$	MPa	400	1146
H	-	1	1
q	-	0.7	0.7
b	-	0.001	0.001
Q	GPa	5276	1704

Fig. 6. Deformation diagram for the different γ' volume fractions.

Influence of the superalloy microstructure evolution on the creep. In this study the high temperature creep of the single-crystal nickel-base superalloy at different stages of microstructure evolution during *rafting* is considered. It is assumed that coalescence of particles of gamma phase has a diffusion character [13]. Three typical stages of alloy morphology changing are analyzed: the initial stage of evolution (particles have a cubical form) with vertical h and horizontal w thickness of γ phase equal to 0.067 μm; the transitional stage of evolution (distance between the γ' particles in perpendicular to loading direction is decreased by a half) with $h = 0,129$ μm and $w = 0,033$ μm; the final stage of evolution, at which the particles γ' are fused, with $h = 0,180$ μm and $w = 0$ μm. The FE models of RVE corresponding to the described above rafting stages are shown in Fig. 7. It is assumed that the loading is applied in the vertical direction.
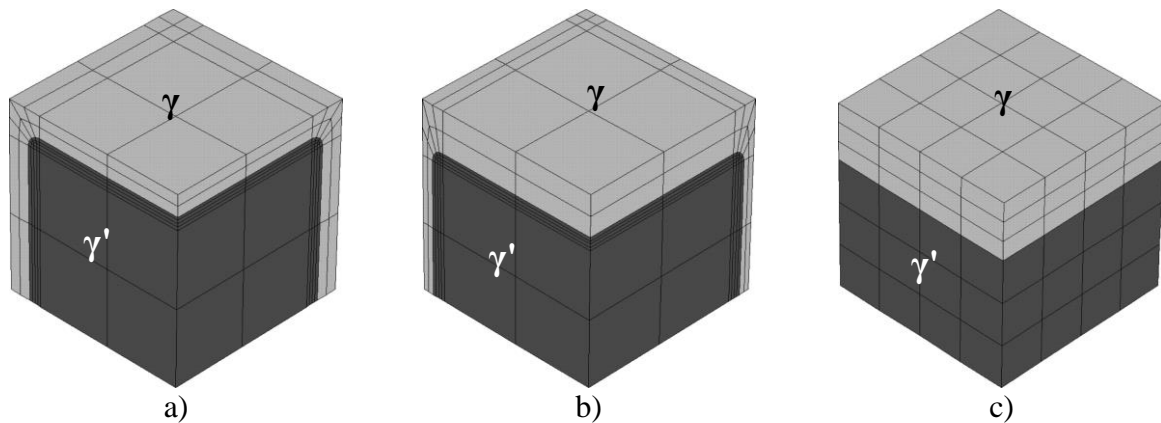

Fig. 7. FE models of nickel-base superalloy RVE for different stages of microstructure evolution: a) γ'-particles have a cubic form, b) distance between the γ'-particles in perpendicular to the loading direction is decreased by a half, c) the γ'-particles are fused.

Multivariant computational experiments show that the microctructure evolution during rafting process under high temperature creep leads to increasing the creep rate. Fig. 8 presents the creep curves for the different stages of microstructure evolution. The obtained results of FE simulations for the creep behavior have demonstrated a good qualitative agreement with experimental data for the durability [14].

Obtained results point out on the possibility to apply the proposed approach for the analysis of stress-strain state of the single-crystal nickel-based alloys with account of the rafting processes under high temperature creep.
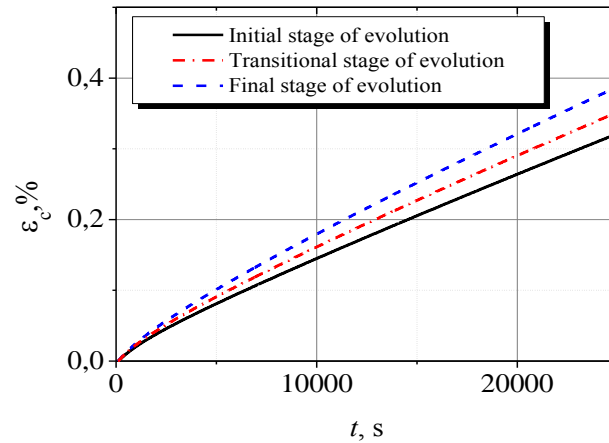
Fig. 8. Creep curves for three different stages (see RVE in Fig. 7) of microstructure evolution.

References
[1] T.M. Pollock, S. Tin // *Journal of Propulsion and Power* **22(2)** (2006) 361.
[2] E.A. Tikhomirova, A.I. Rybnikov, L.B. Getsov // *Metal Science and Heat Treatment* (2016) to be published.
[3] D.W. Maclachlan, D.M. Knowles // *Fatigue & Fracture of Engineering Materials & Structures* **25** (2002) 399.
[4] A.S. Semenov, L.B. Getsov // *Strength of Materials* **46(1)** (2014) 38.
[5] L.B. Getsov, A.S. Semenov, In: *Proceedings of NPO CKTI, N 296, Strength of Materials and Resource Elements of Power (*St. Petersburg, 2009), p. 83.
[6] A.S. Semenov // *St. Petersburg State Polytechnical University Journal* **194(2)** (2014) 15.
[7] A.S. Semenov, L.B. Getsov, S.G. Semenov, A.I. Grishchenko // *Vestnik of the Samara State Aerospace University* **47(5) (**2014) 70.
[8] R. Estevez, G. Hoinard, P. Franciosi // *Acta Materialia* **45** (1997) 1567.
[9] E.P. Busso, F.T. Meissonnier, N.P. O'Dowd // *Journal of the Mechanics and Physics of Solids* **48** (2000) 2333.
[10] J. Besson, G. Cailletaud, J.-L. Chaboche, S. Forest, *Non-Linear Mechanics of Materials* (St. Petersburg, 2010).
[11] U.F. Kocks, T.J. Brown // *Acta Materialia* **14** (1966) 87.
[12] A.S. Semenov, In: *Proceedings of the Vth International Conference on Engineering Problems of Predicting the Reliability and Service Life of Structures*, ed. by B.E. Melnikov (2003), p. 466.
[13] A.I. Epishin, I.L. Svetlov, Y.I. Brueckner // *Materials Science* **5** (1999) 32.
[14] M. Kamaraj // *Sadhana* **28** (2003) 115.